Chapter 2
Intelligent Behaviour Modelling and Control for Mobile Manipulators

Ayssam Elkady, Mohammed Mohammed, Eslam Gebriel, and Tarek Sobh

Abstract In the last several years, mobile manipulators have been increasingly utilized and developed from a theoretical viewpoint as well as for practical applications in space, underwater, construction and service environments. The work presented in this chapter deals with the problem of intelligent behaviour modelling and control of a mobile manipulator for the purpose of simultaneously following desired end-effector and platform trajectories. Our mobile manipulator comprised a manipulator arm mounted on a motorized mobile base wheelchair. The need for accurate modelling of the mobile manipulator is crucial in designing and controlling the motion of the robot to achieve the target precision and manipulability requirements. In this chapter, we propose a new method for measuring the manipulability index used for serial manipulators. Furthermore, we provide some simulations that are implemented on different serial manipulators, such as the Puma 560 manipulator, a six degrees of freedom (DOF) manipulator and the Mitsubishi Movemaster manipulator. We then extend the manipulability concept commonly used for serial manipulators to general mobile manipulator systems.

Keywords Mobile manipulator · Manipulability · Jacobian · Dexterity · Singular value decomposition · Singularities · Nonholonomic · Kinematics

2.1 Introduction

Studying the performance characteristics of the robot, such as dexterity, manipulability and accuracy, is very important to the design and analysis of a robot manipulator. The manipulability is the ability to move in arbitrary directions, while the accuracy is a measure of how close the manipulator can return to a previously taught point. The workspace of a manipulator is a total volume swiped out by the end effector when it executes all possible motions. The workspace is subdivided into the reachable workspace and the dexterous workspace. The reachable

A. Elkady (✉)
University of Bridgeport, Bridgeport, CT 06604, USA
e-mail: ayssam.elkady@gmail.com

A.-E. Hassanien et al. (eds.), *Pervasive Computing: Innovations in Intelligent Multimedia and Applications*, Computer Communications and Networks,
DOI 10.1007/978-1-84882-599-4_2,

workspace is all point reachable by the end-effector. But the dexterous workspace consists of all points that the end-effector can reach with an arbitrary orientation of the end-effector. Therefore, the dexterous workspace is a subset of the reachable workspace. The dexterity index is a measure of a manipulator to achieve different orientations for each point within the workspace.

In this chapter, we present a new method for measuring the manipulability index, and some simulations are implemented on different manipulators, such as the Puma 560 manipulator, a six degrees of freedom (DOF) manipulator and the Mitsubishi Movemaster manipulator. In addition, we describe how the manipulability measure is crucial in performing intelligent behaviour tasks. The manipulability index is considered as a quantitative and performance measure of the ability for realizing some tasks. This measure should be taken into consideration in the design phase of a serial robot and also in the design of control algorithms. Furthermore, we use the proposed method for measuring the manipulability index in serial manipulators to generalize the standard definition of the manipulability index in the case of mobile manipulators.

2.2 Prior Work

Klein and Blaho [6] proposed some measures for the dexterity of manipulators, then they compared several measures for the problems of finding an optimal configuration for a given end-effector position, finding an optimal workpoint and designing the optimal link lengths of an arm. They considered four measures for dexterity: determinant, condition number, minimum singular value of the Jacobian and joint range availability. Salisbury and Craig [8] illustrated hand designs with particular mobility properties. In addition, they gave a definition of accuracy points within manipulator workspace. They used another performance index which is the condition number of the Jacobian. Yoshikawa [13] gave one of the first mathematical measures for the manipulability of any serial robot by discussing the manipulating ability of robotic mechanisms in positioning and orienting end-effectors. He introduced the term manipulability, which involves the Jacobian and its transpose; then the evaluation of the determinant of the Jacobian can be used to determine the manipulability measure. Gosselin [3] presented two dexterity indices for planar manipulations, the first one is based on a redundant formulation of the velocity equations and the second one is based on the minimum number of parameters. Then the corresponding indices were derived for spatial manipulators. These indices are based on the condition number of the Jacobian matrix of the manipulators. He considered the dexterity index, manipulability, condition number and minimum singular value, then he applied these indexes to a SCARA type robot. Van den Doel and Pai [12] introduced a performance measure of robot manipulators in a unified framework based on differential geometry. The measures are applied to the analysis of two- and three-link planar arm. In [5], the authors demonstrated that manipulability of a mechanism is independent of task space coordinates. Furthermore, they provided a proof of the independency of the manipulability index on the first DOF. In [7], the author

examined two geometric tools for measuring the dexterousness of robot manipulators, manipulability ellipsoids and manipulability polytopes. He illustrated that the manipulability ellipsoid does not transform the exact joint velocity constraints into task space and so may fail to give exact dexterousness measure and optimal direction of motion in task space. Furthermore, he proposed a practical polytope method that can be applied to general 6-dimensional task space.

In [10], Sobh and Toundykov presented a prototyping software tool which runs under the mathematica environment and automatically computes possible optimal parameters of robot arms by applying numerical optimization techniques to the manipulability function, combined with distances to the targets and restrictions on the dimensions of the robot.

Nearly all of the above techniques start by getting the forward kinematics, then the Jacobian equation, which relates to the velocity of the end-effector and the joint velocities.

2.3 Manipulability Measure

2.3.1 Jacobian Matrix

The Jacobian matrix provides a transformation from the velocity of the end-effector in cartesian space to the actuated joint velocities as shown in equation (2.1)

$$\dot{x} = J\dot{q}, \tag{2.1}$$

where $\dot{q}$ is an m-dimensional vector that represents a set of actuated joint rates, $\dot{x}$ is an n-dimensional output velocity vector of the end-effector and J is the $m \times n$ Jacobian matrix. It is possible that $m \neq n$. As an example, a redundant manipulator can have more than six actuated joints, while the end-effector will at most have six DOF, so that $m > n$.

In the singular position, the Jacobian matrix J looses rank. This means that the end-effector looses one or more degrees of twist freedom (i.e., instantaneously, the end-effector cannot move in these directions). The mathematical discussion of singularities relies on the rank of the Jacobian matrix J, which, for a serial manipulator with n joints, is a $6 \times n$ matrix. For a square Jacobian, $\det(J) = 0$ is a necessary and sufficient condition for a singularity to appear.

2.3.2 Singular Value Decomposition Method

The singular value decomposition (SVD) method works for all possible kinematic structures (i.e., with every Jacobian matrix J with arbitrary dimensions $m \times n$). The SVD decomposition of any matrix J is on the form:

$$J_{m\times n} = U_{m\times m}\,\Sigma_{m\times n}\,V^{t}_{n\times n}, \tag{2.2}$$

with

$$\Sigma = \begin{pmatrix} \sigma_1 & 0 & 0 & \dots & 0 & 0 & \dots & 0 \\ 0 & \sigma_2 & 0 & \dots & 0 & 0 & \dots & 0 \\ 0 & 0 & \ddots & 0 & \dots & 0 & \dots & 0 \\ 0 & 0 & \dots & \sigma_{m-1} & 0 & 0 & \dots & 0 \\ 0 & 0 & \dots & 0 & \sigma_m & 0 & \dots & 0 \end{pmatrix}.$$

Such that U and V are orthogonal matrices. Thus,

$$U^t U = I_{m \times m}, \tag{2.3}$$

$$V^t V = I_{n \times n}, \tag{2.4}$$

where I is the identity matrix and the singular values are in descending orders $\sigma_1 \geq \sigma_2 \geq \cdots \geq \sigma_m$. The matrix has a zero determinant and is, therefore, singular (it has no inverse). The matrix has two identical rows (or two identical columns). In other words, the rows are not independent. If one row is a multiple of another, then they are not independent, and the determinant is zero. (Equivalently: If one column is a multiple of another, then they are not independent, and the determinant is zero.) The rank of a matrix is the maximum number of independent rows (or the maximum number of independent columns). A square matrix $A_{n \times n}$ is nonsingular only if its rank is equal to n. Mathematically, matrix J having a full rank means that the rank of $J = m$. In this case, $\sigma_m \neq 0$. When $\sigma_m \approx 0$, the matrix J does not have a full rank, which means that the matrix J looses one or more DOF. This happens physically, when the serial robot has two joint axes coinciding on each other.

2.3.3 Manipulability Measures

Yoshikawa [13] defined the manipulability measure μ as the square root of the determinant of the product of the manipulator Jacobian by its transpose

$$\mu = [\det(J \cdot J^t)]^{1/2}. \tag{2.5}$$

If the Jacobian matrix J is a square matrix, the manipulability μ is equal to the absolute value of the determinant of the Jacobian. Using the SVD, the manipulability can be written as follows:

$$\mu = \sigma_1 \sigma_2 \dots \sigma_m. \tag{2.6}$$

Another method for the manipulability measure is the reciprocal of the condition number [termed the conditioning index] that was used in [11].

2.3.4 *Optimizing the Manipulability Index of Serial Manipulators Using the SVD Method*

Our current work addresses the manipulability index for every point within the workspace of some serial manipulators. The method provided promising results, since it is considered one of the crucial tasks required for designing trajectories or avoiding singular configurations. We propose a new method for measuring the manipulability, then we implemented simulations supporting our method on the Puma 560 manipulator, a six DOF manipulator and the Mitsubishi Movemaster manipulator. As mentioned in [11], the determinant of a Jacobian cannot be used for expressing the manipulability's index. It reaches zero when a manipulator reaches any singular configuration. Another method has been proposed, labelled the reciprocal of the Jacobian (as in [11]). In past researches, there was an argument about whether the minimum value of the σ's in (2.2) or the multiplication of all σ's exactly represents the manipulability's index [3].

In this work, we propose a new concept for measuring this index, then justify this concept by visualizing the bands of this index, resulting from our experiments. Moreover, a new relationship between the minimum rank of the Jacobian matrix and the order of one of these σ's (in (2.2)) can exactly express the manipulability's index.

2.3.4.1 The Puma 560 Manipulator: A Case Study

In case of the singular configuration of the Puma 560 manipulator at $Q = [0, 0, -\frac{\pi}{2}, 0, 0, 0]$, the following would be the J, U, Σ and V matrices as depicted in (2.2):

$$J = \begin{bmatrix} 0 & 0 & 0 & 0 & 0 & 0 \\ 20 & 0 & 0 & 0 & 0 & 0 \\ 0 & 20 & 10 & 0 & 0 & 0 \\ 0 & 0 & 0 & 1 & 0 & 1 \\ 0 & 1 & 1 & 0 & 1 & 0 \\ 1 & 0 & 0 & 0 & 0 & 0 \end{bmatrix},$$

$$U = \begin{bmatrix} 0 & 0 & 0 & 0 & 1 & -0.0034 \\ 0 & -0.9988 & 0 & 0 & -0.0002 & -0.0499 \\ -0.9982 & 0 & 0 & 0.06 & 0 & 0 \\ 0 & 0 & -1 & 0 & 0 & 0 \\ 0.06 & 0 & 0 & 0.9982 & 0 & 0 \\ 0 & -0.0499 & 0 & 0 & 0.0034 & 0.9987 \end{bmatrix},$$

$$\Sigma = \begin{bmatrix} 22.401 & 0 & 0 & 0 & 0 & 0 \\ 0 & 20.025 & 0 & 0 & 0 & 0 \\ 0 & 0 & 1.4142 & 0 & 0 & 0 \\ 0 & 0 & 0 & 1.0935 & 0 & 0 \\ 0 & 0 & 0 & 0 & 0 & 0 \\ 0 & 0 & 0 & 0 & 0 & 0 \end{bmatrix},$$

$$V = \begin{bmatrix} 0 & -1 & 0 & 0 & 0 & 0 \\ -0.8939 & 0 & 0 & 0.1852 & 0.4074 & -0.027 \\ -0.4483 & 0 & 0 & -0.3638 & -0.8147 & 0.0539 \\ 0 & 0 & -0.7071 & 0 & -0.0467 & -0.7056 \\ -0.0027 & 0 & 0 & -0.9129 & 0.4074 & -0.027 \\ 0 & 0 & -0.7071 & 0 & 0.0467 & 0.7056 \end{bmatrix}.$$

It is obvious that in the singular matrix Σ, σ_5 and σ_6 assume the value zero with small tolerance. This is due to the fact that there are two singular cases in its configuration; the fourth and sixth joints are on same axis and it is in a singular arm configuration, and thus, σ_5 is zero.

2.3.5 *Proposed Manipulability Measure Algorithm*

To justify the proposed method, the following algorithm is proposed:

Algorithm 1: Calculate the manipulability index

1: Find the joint(s) that may lead to a singular configuration assuming that the number of these joints $= n$.
2: **for** $i = 1$ to n **do**
3: Change the value of the i^{th} joint from its initial to its final value using simulation software – Matlab robotic toolbox [2] is used in our case.
4: Calculate the Jacobian (J) and singular (Σ) matrix.
5: Plot every normalized σ and also the rank of the Jacobian matrix.

$$\text{Normalized}\sigma_i = \frac{\sigma_i}{Max\{\sigma_{i1,}\sigma_{i2}, \sigma_{i3}, ..., \sigma_{in}\}} \tag{2.7}$$

Where: i is the order of the σ in the singular matrix and n is the number of steps during the simulation.
6: Check the rank of the Jacobian matrix.
7: **end for**

2.4 Experiments

In this section, we will show and explain some results using serial manipulators with DH parameters illustrated in Tables 2.1–2.3. We have proposed some assumptions which can be summarized as follows:

- In our case study, we have dealt with the arm manipulability regardless of the orientation singularity.
- We study non-redundant manipulators only.

2.4.1 The Puma 560 Manipulator

In the Puma 560, we have experienced that the third joint is the cause of singularity. The sample trajectory of this manipulator from the initial position $Q_{\text{initial}} = [0, 0, -\frac{\pi}{2}, 0, 0, 0]$ to the final position $Q_{\text{final}} = [0, 0, \frac{\pi}{2}, 0, 0, 0]$ is shown in Fig. 2.1. The DH parameters of the Puma 560 are shown in Table 2.1.

Table 2.1 DH parameters of the Puma 560 manipulator

i	α	a	θ	d	Initial limit	Final limit	Joint's type
1	90	0	*	0	−170	170	*R*
2	0	0.4318	*	0	−225	45	*R*
3	−90	0.0203	*	0.15005	−250	75	*R*
4	90	0	*	0.4318	−135	100	*R*
5	−90	0	*	0	−100	100	*R*
6	0	0	*	0	−180	180	*R*

Table 2.2 DH parameters of a six degrees of freedom (DOF) serial manipulator

i	α	a	θ	d	Initial limit	Final limit	Joint's type
1	90	0	*	10	−170	170	*R*
2	0	10	*	0	−225	45	*R*
3	−90	0	*	0	−250	75	*R*
4	90	0	*	10	−135	100	*R*
5	−90	0	*	0	−100	100	*R*
6	0	0	*	0	−180	180	*R*

Table 2.3 Manipulability's bands of the Mitsubishi Movemaster manipulator in 2D workspace

i	α	a	θ	d	Initial limit	Final limit	Joint's type
1	90	0	*	300	−150	150	*R*
2	0	250	*	0	100	130	*R*
3	0	160	*	0	−110	0	*R*
4	−90	0	*	0	−90	90	*R*
5	0	0	*	72	0	0	*R*

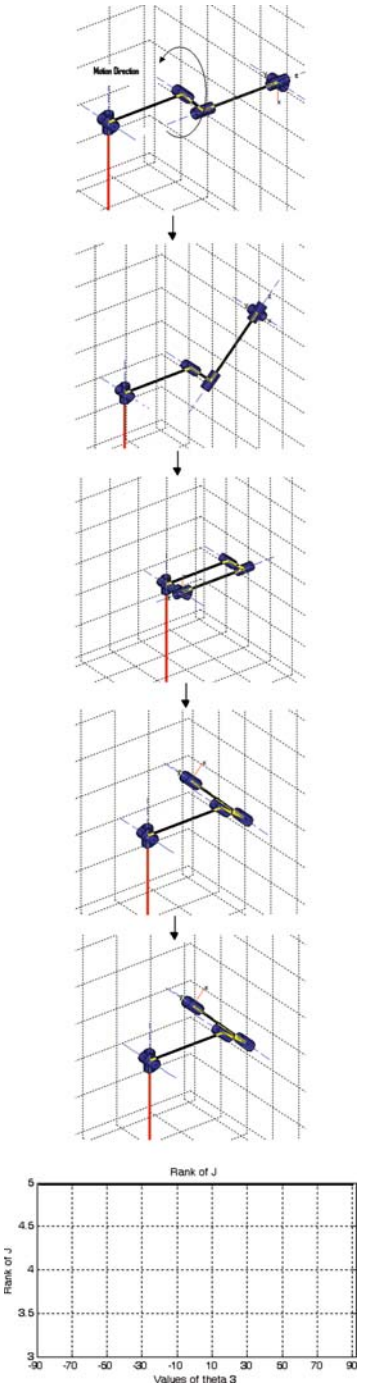

Fig. 2.1 Phases for the Puma 560 manipulator, changing from the initial singular configuration to the final singular configuration with the corresponding rank

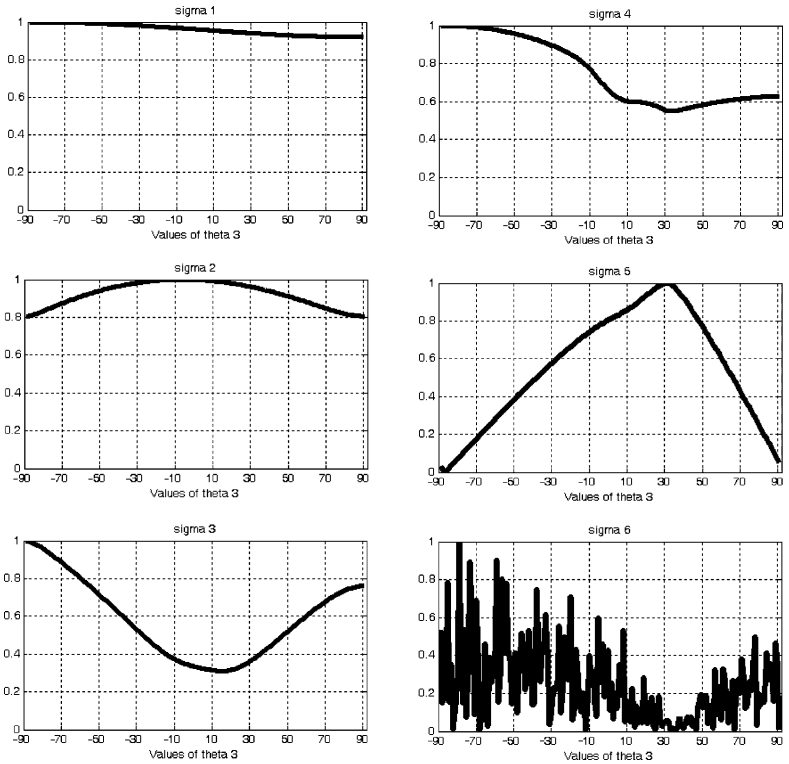

Fig. 2.2 The behaviour of σ_1 to σ_6 during the experiment

In Fig. 2.2, it is obvious that σ_5 is exactly expressing the manipulability's index. Furthermore, the rank of the Jacobian matrix during this experiment was constant at 5 because joints 6 and 4 were on same axis during the whole experiment. The manipulability index of every point within the whole workspace is represented in bands and each band is visualized using a different color as shown in Fig. 2.3.

Figure 2.3 is considered important in our research strategy since it provides a visual demonstration for the manipulability measure for the entire workspace for the Puma 560 manipulator. These results can strongly contribute in developing an intelligent mobile manipulator. For example, the positions with the highest manipulability index will have better dexterity compared with those of the lowest manipulability index.

2.4.2 A Six Degrees of Freedom Serial Manipulator

Similarly, we implemented the same procedure for the Mitsubishi Movemaster manipulator and a regular six DOF manipulator. In a six DOF manipulator, the sample

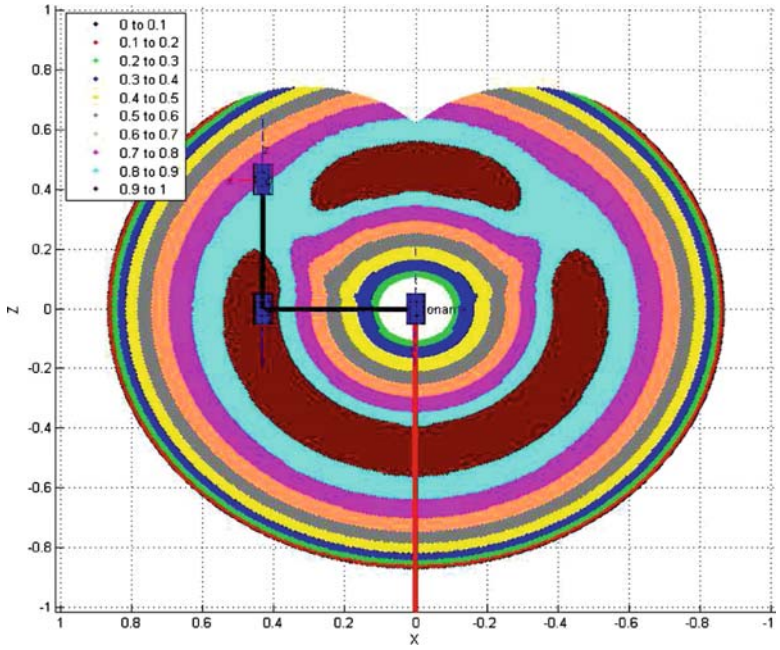

Fig. 2.3 Manipulability's bands of the puma 560 manipulator in 2D workspace according to σ_5

trajectory of this manipulator is from the initial position $Q_{\text{initial}} = [0, 0, -\frac{\pi}{2}, 0, 0, 0]$ to the final position $Q_{\text{final}} = [0, 0, \frac{\pi}{2}, 0, 0, 0]$. The DH parameters of this manipulator are shown in Table 2.2. The behaviour of σ_3 during the experiment is shown in Fig. 2.4. The visual demonstration of the manipulability index is shown in Fig. 2.5.

2.4.3 The Mitsubishi Movemaster Manipulator

The initial position is $Q_{\text{initial}} = [0, 0, -\frac{\pi}{2}, 0, 0, 0]$ and the final position $Q_{\text{final}} = [0, 0, \frac{\pi}{2}, 0, 0, 0]$. The DH parameters of this manipulator are shown in Table 2.3. The behaviour of σ_3 during the experiment is shown in Fig. 2.6. The visual demonstration of the manipulability index is shown in Fig. 2.7.

2.4.4 Experimental Results

It is obvious from Table 2.4 that we can suppose that the order of σ that is expressing the kinematics manipulability's index equals to the minimum rank of the Jacobian matrix.

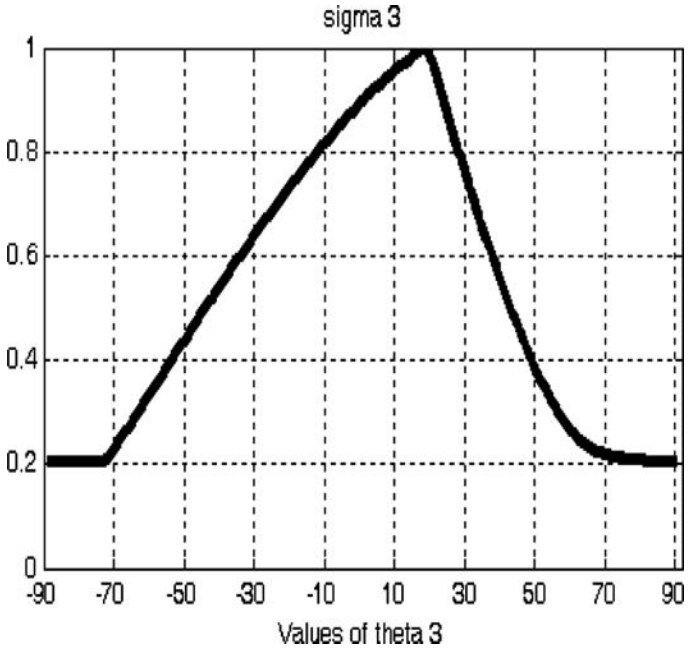

Fig. 2.4 The behaviour of σ_3 during the experiment

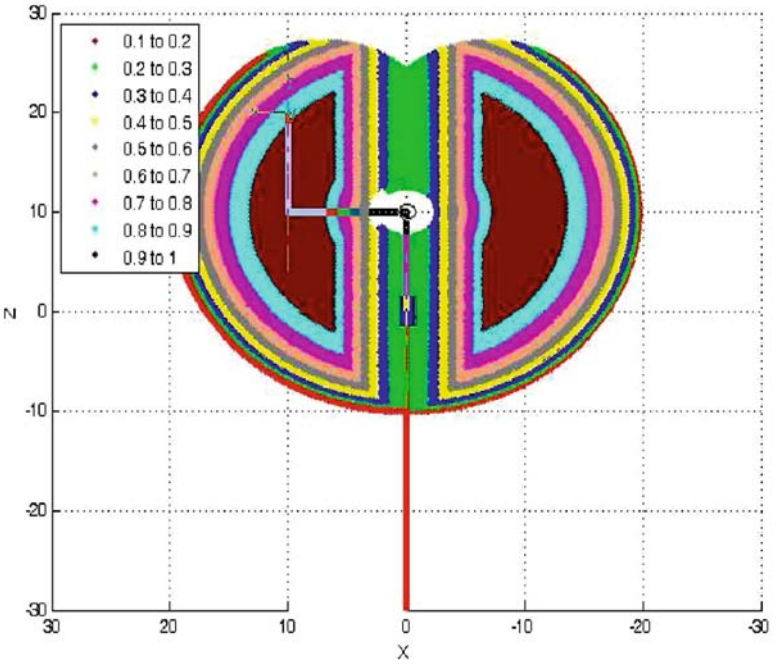

Fig. 2.5 Manipulability's bands of a six degrees of freedom (DOF) manipulator 2D

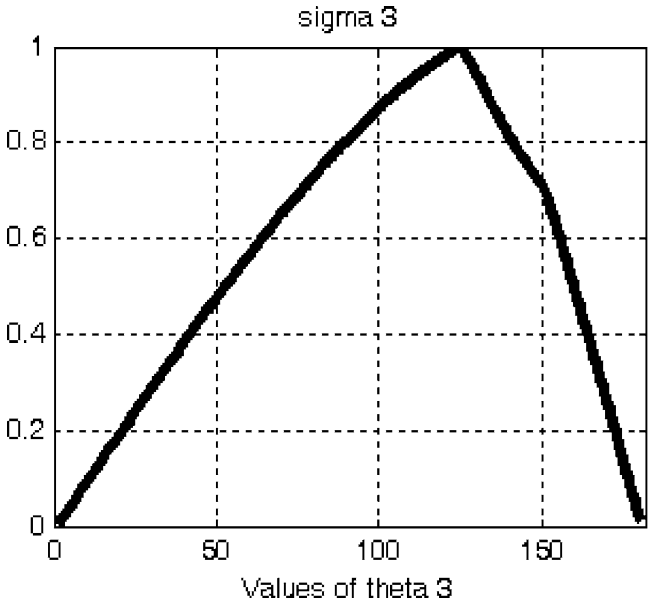

Fig. 2.6 The behaviour of σ_3 during the experiment

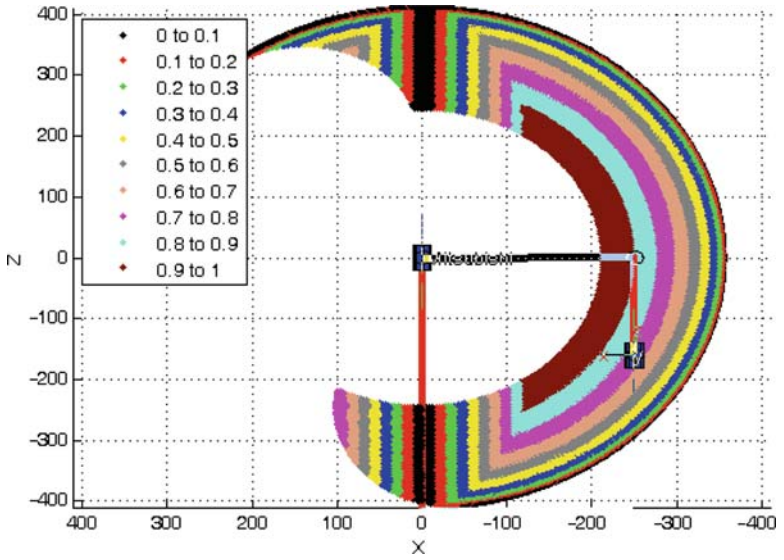

Fig. 2.7 Manipulability's bands of the Mitsubishi Movemaster manipulator in 2D workspace

Table 2.4 Summary of results

Manipulator	Order of σ expressing the manipulability	Min rank of the Jacobian matrix
Puma 560	5	5
Six DOF	3	3
Mitsubishi movemaster	3	3

2.5 Mobile Manipulator

A mobile manipulator is a manipulator mounted on a mobile platform with no support from the ground. A mobile manipulator offers a dual advantage of mobility offered by the platform and dexterity offered by the manipulator. For instance, the mobile platform extends the workspace of the manipulator. The DOF of the mobile platform also adds to the redundancy of the system. The mobile manipulator is required to perform complicated tasks and is potentially useful in dangerous and unpredictable environments, such as at a construction site, space, underwater, construction, service environments and in nuclear power station. Arai [1] suggested that the mobile manipulator system should be capable of both locomotion and manipulation when it is applied to various tasks in construction, agriculture, home, office and hospital services. Then he described why and how locomotion and manipulation should be integrated, what the benefits are and what problems must be solved in terms of practical application of the robot. In [9], a systematic modelling of the nonholonomic mobile manipulators is proposed. The derived models are used to generalize the standard definition of manipulability to the case of mobile manipulators. In addition, the effects of mounting a robotic arm on a nonholonomic platform were shown through the analysis of the manipulability.

In fixed based serial manipulators, manipulability depends on link lengths, joint types, joint motion limits and the structure of the manipulator. In mobile manipulator, the manipulability depends on the kinematics, geometric design, the payload and mass and mass distribution of the mobile platform. Thus, the manipulability measure in mobile manipulators is very complicated due to the coupling between the kinematic parameters and the dynamics effect.

We extend the manipulability concept commonly used for serial manipulators to general mobile manipulator systems. To study the manipulability and dexterity measure for a mobile manipulator, we first study those of the fixed base serial manipulator as discussed in the previous sections.

2.6 RISC Mobile Manipulator

We are developing and constructing the mobile manipulator platform RISC. The prototype of the RISC is shown in Fig. 2.8. The RISC mobile manipulator has been designed to support our research in algorithms and control for autonomous mobile

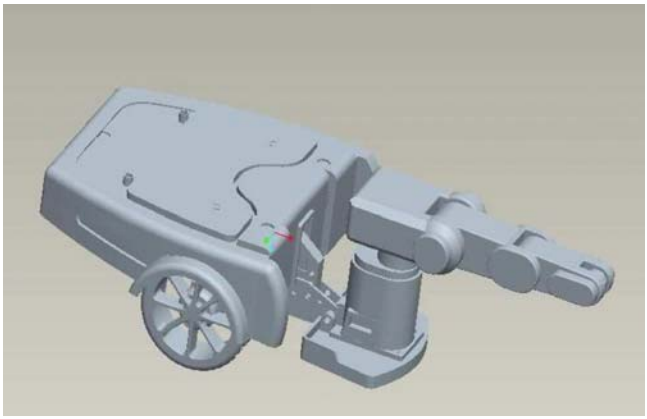

Fig. 2.8 A prototype of the RISC manipulator

manipulator. The objective is to build a hardware platform with redundant kinematic DOF, a comprehensive sensor suite and significant end-effector capabilities for manipulation. The RISC platform differs from any related robotic platforms because its mobile platform is a wheelchair base. Thus, the RISC has the advantages of the wheelchair, such as high payload, high speed motor package (the top speed of the wheelchair is 6 miles/h), Active-Trac and rear caster suspension for outstanding outdoor performance and adjustable front anti-tips to meet terrain challenges.

2.7 Modelling of the RISC

2.7.1 The Position of the Robot

In order to specify the position of the robot on the plane, we establish a relationship between the global reference frame of the plane and the local reference frame of the robot. The origin O of the global reference frame is selected at arbitrary on the plane as shown in Fig. 2.9. The point C is the centre of mass of the robot. The origin P of the local reference frame of the robot $\{X_p,Y_p\}$ is at the centre of the robot. The basis defines two axes relative to P on the robot chassis and is, thus, the robot's local reference frame. The position of P in the global reference frame is specified by coordinates x and y and the angular difference between the global and local reference frames is given by θ. The pose of the robot is described by a vector ξ.

$$\xi = \begin{bmatrix} x \\ y \\ \theta \end{bmatrix}. \tag{2.8}$$

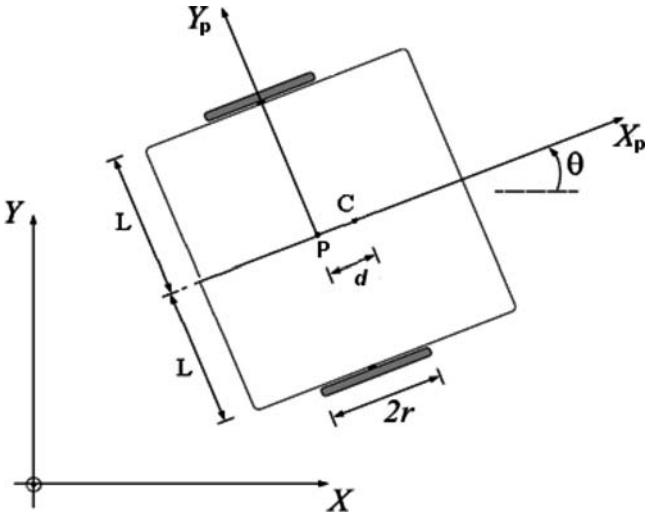

Fig. 2.9 Kinematic model of the RISC

To describe the robot's motion, it will be necessary to map the motion along the axes from the global reference frame to the robot's local reference frame. This mapping is accomplished using the orthogonal rotation matrix $R(\theta)$, where

$$R(\theta) = \begin{bmatrix} \cos(\theta) & \sin(\theta) & 0 \\ -\sin(\theta) & \cos(\theta) & 0 \\ 0 & 0 & 1 \end{bmatrix}.$$

This orthogonal rotation $R(\theta)$ is used to map the motion ξ in the global reference frame to motion ${}^{P}\xi$ in terms of the local reference frame $\{X_p, Y_p\}$. This operation is:

$${}^{P}\xi = R(\theta)\xi \tag{2.9}$$

2.7.2 The velocity of the robot

Given that the spinning speed of left wheel is $\dot{\Phi}_l$ and the spinning speed of the right wheel is $\dot{\Phi}_r$, a forward kinematic model would predict the robot's overall speed in the global reference frame. The linear velocity of the centre of the right wheel is v_r, where

$$v_r = r\dot{\Phi}_r. \tag{2.10}$$

In addition, the velocity of the left one is v_l where

$$v_l = r\dot{\Phi}_l. \tag{2.11}$$

Using the instantaneous centre of rotation (ICR), if the linear velocity of the centre P of the robot is V and its angular velocity ω, we can find that:

$$V = \frac{v_r + v_l}{2}, \tag{2.12}$$

$$\omega = \dot{\theta} = \frac{v_r - v_l}{2L}. \tag{2.13}$$

The velocity of point P in its local reference frame ${}^{P}\dot{\xi}_p$:

$${}^{P}\dot{\xi}_p = \begin{bmatrix} V \\ 0 \\ \dot{\theta} \end{bmatrix}. \tag{2.14}$$

The velocity of point C in the local reference frame $\{X_p, Y_p\}$ is ${}^{P}\dot{\xi}_c$ where

$${}^{P}\dot{\xi}_c = \begin{bmatrix} V \\ \dot{\theta} d \\ \dot{\theta} \end{bmatrix}. \tag{2.15}$$

The velocity of point P in the global reference frame $\dot{\xi}_p$ is

$$\dot{\xi}_p = R(\theta)^{-1}\, {}^{P}\dot{\xi}_p, \tag{2.16}$$

$$\dot{\xi}_p = \frac{r}{2} \begin{bmatrix} (\dot{\Phi}_l + \dot{\Phi}_r)\cos(\theta) \\ (\dot{\Phi}_l + \dot{\Phi}_r)\sin(\theta) \\ \frac{(\dot{\Phi}_r - \dot{\Phi}_l)}{l} \end{bmatrix}. \tag{2.17}$$

The velocity of point C in the global reference frame $\dot{\xi}_c$ is

$$\dot{\xi}_c = R(\theta)^{-1}\, {}^{P}\dot{\xi}_c. \tag{2.18}$$

Thus,

$$\dot{\xi}_c = \begin{bmatrix} \dot{x}_c \\ \dot{y}_c \\ \dot{\theta} \end{bmatrix} = \frac{r}{2} \begin{bmatrix} (\dot{\Phi}_l + \dot{\Phi}_r)\cos(\theta) + \frac{d}{l}(\dot{\Phi}_l - \dot{\Phi}_r)\sin(\theta) \\ r(\dot{\Phi}_l + \dot{\Phi}_r)\sin(\theta) + \frac{d}{l}(\dot{\Phi}_r - \dot{\Phi}_l)\cos(\theta) \\ \frac{(\dot{\Phi}_r - \dot{\Phi}_l)}{l} \end{bmatrix}. \tag{2.19}$$

2.7.3 Kinematic Constraints

However, several important assumptions will simplify this representation. First, the plane of the wheel always remains vertical and that there is, in all cases, one single point of contact between the wheel and the ground plane. Furthermore, there is no sliding at this single point of contact, so the wheel undergoes motion only under conditions of pure rolling and rotation about the vertical axis through the contact point.

The fixed standard wheel has no vertical axis of rotation for steering. Its angle to the chassis is fixed and it is limited to back and forth motion along the wheel plane and rotation around its contact point with the ground plane. The rolling constraint for this wheel enforces that all motions along the direction of the wheel plane must be accompanied by the appropriate amount of wheel spin. Thus, the first constraint is

$$\dot{y}_c \cos(\theta) - \dot{x}_c \sin(\theta) - \dot{\theta} d = 0. \tag{2.20}$$

Furthermore, there are two rolling constraints, i.e., the driving wheels do not slip,

$$\dot{x}_c \cos(\theta) + \dot{y}_c \sin(\theta) + \dot{\theta} l = r\dot{\Phi}_r, \tag{2.21}$$

$$\dot{x}_c \cos(\theta) + \dot{y}_c \sin(\theta) - \dot{\theta} l = r\dot{\Phi}_l. \tag{2.22}$$

Letting $q = [x_c y_c, \theta, \Phi_r, \Phi_l]^t$, the three constraints can be written in the form of:

$$A(q)\dot{q} = 0, \tag{2.23}$$

where

$$A(q) = \begin{bmatrix} \sin\theta & -\cos\theta & d & 0 & 0 \\ \cos\theta & \sin\theta & l & -r & 0 \\ -\cos\theta & -\sin\theta & l & 0 & r \end{bmatrix} \quad \text{and} \quad \dot{q} = \begin{bmatrix} \dot{x}_c \\ \dot{y}_c \\ \dot{\theta} \\ \dot{\phi}_r \\ \dot{\phi}_l \end{bmatrix}.$$

The last two equations are called the nonholonomic constraint because they are not integrable differential equations.

2.8 Conclusions and Future Work

In this chapter, we present a new algorithm for measuring manipulability, and then we implement simulations supporting our methodology on different manipulators. We describe how mobile manipulator capabilities are a key to several robotic applications and how the manipulability measure is crucial in performing intelligent behaviour tasks such as grasping, pulling or pushing objects with sufficient dexterity.

In our anticipated future work, there will be an ongoing effort for the development of multiple mobile manipulator systems and platforms, which will interact with each other to perform more complex tasks exhibiting intelligent behaviours utilizing the proposed manipulability measure.

References

1. T. Arai (1996) Robots with integrated locomotion and manipulation and their future. Proceedings of the 1996 IEEE/RSJ International Conference on Robots and Intelligent Systems, IROS 96, vol. 2, Osaka, pp. 541–545.
2. P.I. Corke (2002) Robotic toolbox.
3. C.M. Gosselin (1990) Dexterity indices for planar and spatial robotic manipulators. Proceedings of the International Conference on Robotics and Automation, vol. 1, May 1990, pp. 650–655.
4. C. Gosselin, J. Angeles (1988) The optimum kinematic design of a planar three-degree-of-freedom parallel manipulator. Journal of Mechanisms, Transmissions and Automation in Design 110, 35–41.
5. K. Gotlih, I. Troch (2004) Base Invariance of the Manipulability Index. Robotica archive. Cambridge University Press, New York, NY, USA, 22(4), pp. 455–462.
6. C.A. Klein, B.E. Blaho (1987) Dexterity measures for the design and control of kinematically redundant manipulators. The International Journal of Robotics Research 6(2), 72–83.
7. J. Lee (1997) A study on the manipulability measures for robot manipulators. Intelligent Robots and Systems 3(7–11), 1458–1465.
8. J.K. Salisbury, J.J. Craig (1982) Articulated hands. Force control and kinematic issues. The International Journal of Robotics Research 1(1), 4–17.
9. R. Siegwart, I.R. Nourbakhsh (2004) Intelligent Robotics and Autonomous Agents Series. MIT Press, Cambridge, MA, ISBN 0-262-19502-X.
10. T.M. Sobh, D.Y. Toundykov (2004) Optimizing the tasks at hand. IEEE Robotics and Automation Magazine 11(2), 78–85.
11. T. Tanev, B. Stoyanov (2000) On the Performance Indexes for Robot Manipulators. Problems of Engineering Cybernetics and Robotics.
12. K. van den Doel, D.K. Pai (1996) Performance measures for robot manipulators: A unified approach. The International Journal of Robotics Research 15(1), 92–111.
13. T. Yoshikawa (1985) Manipulability of robotic mechanisms. The International Journal of Robotics Research 4(2), 3–9.